© 2014. Published by The Company of Biologists Ltd | Development (2014) 141, 1526-1533 doi:10.1242/dev.102343

RESEARCH ARTICLE

A novel serotonin-secreting cell type regulates ciliary motility in the mucociliary epidermis of *Xenopus* tadpoles

Peter Walentek[1,*], Susanne Bogusch[1], Thomas Thumberger[1,‡], Philipp Vick[1], Eamon Dubaissi[2], Tina Beyer[1,§], Martin Blum[1] and Axel Schweickert[1,¶]

ABSTRACT

The embryonic skin of *Xenopus* tadpoles serves as an experimental model system for mucociliary epithelia (MCE) such as the human airway epithelium. MCEs are characterized by the presence of mucus-secreting goblet and multiciliated cells (MCCs). A third cell type, ion-secreting cells (ISCs), is present in the larval skin as well. Synchronized beating of MCC cilia is required for directional transport of mucus. Here we describe a novel cell type in the *Xenopus laevis* larval epidermis, characterized by serotonin synthesis and secretion. It is termed small secretory cell (SSC). SSCs are detectable at early tadpole stages, unlike MCCs and ISCs, which are specified at early neurulation. Subcellularly, serotonin was found in large, apically localized vesicle-like structures, which were entirely shed into the surrounding medium. Pharmacological inhibition of serotonin synthesis decreased the velocity of cilia-driven fluid flow across the skin epithelium. This effect was mediated by serotonin type 3 receptor (*Htr3*), which was expressed in ciliated cells. Knockdown of *Htr3* compromised flow velocity by reducing the ciliary motility of MCCs. SSCs thus represent a distinct and novel entity of the frog tadpole MCE, required for ciliary beating and mucus transport across the larval skin. The identification and characterization of SSCs consolidates the value of the *Xenopus* embryonic skin as a model system for human MCEs, which have been known for serotonin-dependent regulation of ciliary beat frequency.

KEY WORDS: Small secretory cell, Serotonin, *Xenopus*, Mucociliary epithelium, Cilia

INTRODUCTION

Besides its role as a neurotransmitter, the monoamine serotonin (5-hydroxytryptamine; 5-HT) displays broad biological functions throughout the animal kingdom. The bulk of serotonin (up to 95%) is synthesized in non-neural tissues, mainly by epithelial cells of the intestine. Tryptophan hydroxylase, the rate-limiting enzyme for serotonin synthesis, is encoded by two closely related genes, *TPH1/2*, which display cell-type-specific expression in non-neural and neural cells, respectively. Serotonin synthesis from 5-hydroxytryptophan is catalyzed by DOPA-decarboxylase (aromatic L-amino acid decarboxylase) (Amireault et al., 2013; Gutknecht et al., 2009). In humans, a number of serotonin-dependent diseases have been described: for example, pulmonary-atrial hypertonia (Berger et al., 2009), irritable bowel syndrome (Mawe et al., 2006) and mental mood disorders such as depression (Berger et al., 2009). Agonistic and antagonistic drugs directed against components of the serotonin pathway present valuable tools to elucidate functional roles of serotonin in different model organisms and, notably, during development as well. In the embryo serotonin signaling was shown to be necessary for heart, bone and gastrointestinal functions in mammals as well as for left-right axis specification in *Xenopus* (Berger et al., 2009; Ducy and Karsenty, 2010; Fukumoto et al., 2005).

A tight relationship between serotonin signaling and cilia function has been described, with serotonin acting on both nonmotile sensory and motile cilia. The serotonin receptor type 6 (5-HT6) on nonmotile neuronal cilia, for example, is thought to measure the amount of serotonin in the extracellular space (Brailov et al., 2000; Whitfield, 2004). The serotonin effect on motile cilia, which are used to move individual cells, whole organisms or extracellular fluids such as mucus and cerebrospinal fluid, can be twofold, via the induction of ciliogenesis or by regulation of ciliary beat frequency (CBF). During left-right axis determination in *Xenopus*, serotonin signaling induces *foxj1* in a Wnt/β-catenin dependent manner (Beyer et al., 2012). *foxj1* in turn governs the formation of motile cilia (Stubbs et al., 2008; Yu et al., 2008). CBF regulation by serotonin signaling has been reported in a range of organisms, from protozoans to mammals (Castrodad et al., 1988; König et al., 2009; Maruyama et al., 1984; Nguyen et al., 2001; Wada et al., 1997; Yoshihiro et al., 1992).

In most cases, the ciliated serotonin-sensitive tissue represents a typical mucociliary epithelium (MCE). MCEs are characterized by the existence of two cell types: multiciliated cells and mucus secreting goblet cells. Synchronized beating of cilia generates directional transport of mucus, which in all cases is of high functional relevance. Flow generated by brain ependymal cilia, for example, generates a gradient of signaling molecules, which governs the direction of neuroblast migration towards the olfactory bulb (Sawamoto et al., 2006). The best-known case certainly is mucociliary clearance of the airway epithelia, which constitutes a first-line defense mechanism against pathogens. Patients suffering from impaired mucus production or cilia function show a high prevalence of lung infections (Albee and Dutcher, 2012; Cowan et al., 2001; Livraghi and Randell, 2007; Rubin, 2007). MCEs must be able to adapt to changing environmental conditions. Cilia-driven flow must be maintained upon altered mucus composition, varying pH, oxygen or water content. As velocity of mucus evacuation is strictly linked to the frequency of ciliary beating (Braiman and Priel, 2008), sensory inputs should be used to regulate CBF, serotonin being but one candidate.

Serotonin-mediated CBF regulation differs between species and tissues, both with respect to receptor type and source of ligand

[1]University of Hohenheim, Institute of Zoology, Garbenstrasse 30, D-70593 Stuttgart, Germany. [2]Faculty of Life Sciences, Michael Smith Building, University of Manchester, Oxford Road, Manchester, M13 9PT, UK.
*Present address: Department of Molecular and Cell Biology, Center for Integrative, Genomics, University of California at Berkeley, Berkeley, California 94720, USA. ‡Present address: Centre for Organismal Studies, Im Neuenheimer Feld 230, Heidelberg University, D-69120 Heidelberg, Germany. §Present address: University Department of Medicine, Department of Sports Medicine, Otfried-Müller-Straße 10, D-72076 Tübingen, Germany.

¶Author for correspondence (axel.schweickert@uni-hohenheim.de)

Received 9 August 2013; Accepted 2 February 2014

Development (2014) doi:10.1242/dev.102343

(Doran et al., 2004; König et al., 2009; Longley and Peterman, 2012; Nguyen et al., 2001). Experimental analysis of mammalian brain and airway MCEs is further hampered by the use of organ cultures from biopsies, which prevents monitoring of long-term effects or complex functional manipulation of multiple pathways. As an alternative, the embryonic skin of early *Xenopus* tadpoles has recently emerged as a novel and accessible experimental model for MCE development and function (Dubaissi and Papalopulu, 2011; Hayes et al., 2007; Stubbs et al., 2012; Wallingford, 2010; Werner and Mitchell, 2012). The epidermis of *Xenopus* embryos, consisting of multiciliated cells (MCCs) as well as goblet cells, produces an anterior-to-posterior flow of extracellular liquid (Hayes et al., 2007; Werner and Mitchell, 2012). A third cell type, ion-secreting cells (ISCs), are characterized by expression of pH regulators ATP6 and carbonic anhydrases (Dubaissi and Papalopulu, 2011; Quigley et al., 2011). The relevance of the *Xenopus* model has been proven by unraveling basic molecular mechanisms and signaling events required for MCE development and function, such as cell-type specification and cilia alignment (Werner and Mitchell, 2012).

Here we report a fourth cell type in the tadpole skin: namely small secretory cells (SSCs). SSCs synthesize and secrete serotonin, which functionally regulates CBF and velocity of mucus transport. SSCs complete the descriptive and functional characterization of the frog MCE and should contribute to the growing relevance of this model system.

RESULTS

A novel serotonin-secreting cell type in the embryonic tadpole skin

As an entry point into the analysis of serotonin function in the ciliated tadpole skin we analyzed serotonin localization and ciliation during embryogenesis, using antibodies against serotonin and acetylated alpha-tubulin. At stage 26 only very few and weak serotonin-positive signals were detected in the deep layer of the skin ectoderm (not shown). Frequency and intensity of signals increased during later development (stages 27-33), showing a punctate pattern in the epidermis (Fig. 1A). Closer examination demonstrated that serotonin-positive signals were localized in the epithelial layer, intermingled with MCCs (Fig. 1A′). Magnification of single serotonin-positive cells revealed the presence of serotonin in vesicle-like structures. Colocalization of serotonin-containing vesicles with cilia was occasionally observed (Fig. 1A″; supplementary material Fig. S1A,B), suggesting that vesicles were released from cells and transported towards MCCs by cilia-driven flow. Serotonin-containing vesicles thus should be enriched at and released from the apical side of cells.

To investigate this possibility, we analyzed the subcellular localization of serotonin-positive vesicles along the apicobasal axis, using phalloidin to stain for actin enrichment at the apical membrane as a reference point. Interestingly, localization of serotonin-containing vesicles was variable, even in neighboring cells (Fig. 1B). Orthogonal virtual sections through *z*-stack series of confocal micrographs of individual cells showed vesicles beneath, at, or considerably above the apical membrane (Fig. 1B′-B‴), suggesting a dynamic sequence of events during vesicle release. Size of vesicles was variable, with a maximum diameter of 2.5 µm (e.g. large vesicle in Fig. 1B‴). SEM analyses of stage 32 tadpoles confirmed the immunofluorescence (IF) results. Cells with an undulated apical membrane, indicating intracellular vesicles beneath the apical membrane, and cells with external vesicles ready to detach were both present in the skin of *Xenopus laevis* (Fig. 1C,C′), as described (Montorzi et al., 2000; Nickells et al., 1988). Supplementary material Fig. S1C shows an orthogonal section through a serotonin-positive cell, based on actin-serotonin double staining in a set of optical sections along the apicobasal axis. This cell is of triangular shape and displays only a small apical surface. Surprisingly, the size of serotonin-positive vesicles was variable along the apicobasal axis and vesicle diameters correlated with the

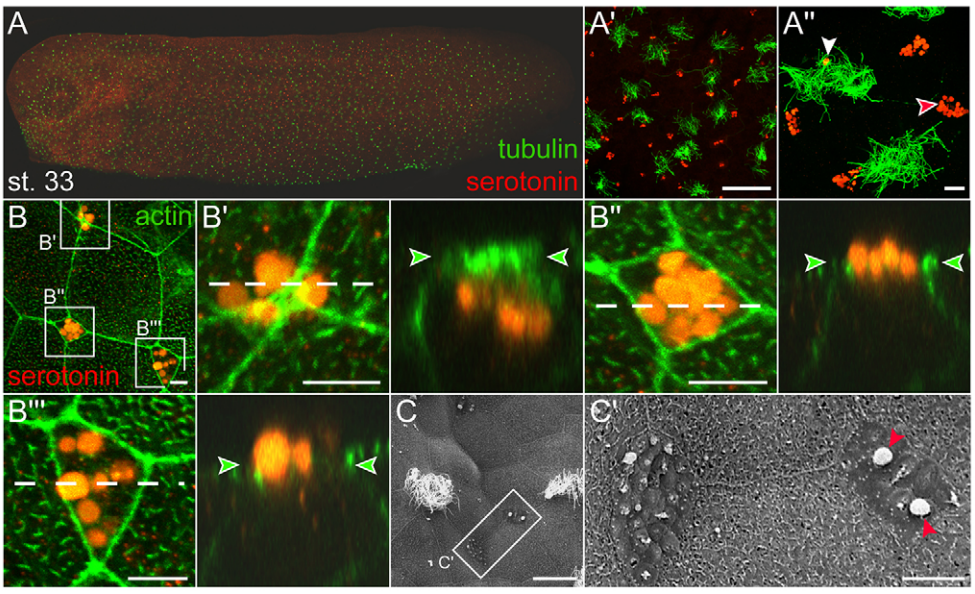

Fig. 1. Small secretory cells (SSCs) in the *Xenopus* tadpole epidermis. (A) Stage 33 tadpole stained for serotonin (red) and cilia (green) using anti-serotonin and anti-acetylated-α-tubulin antibodies. (A′,A″) Higher magnification reveals vesicular nature of serotonin staining. Please note a serotonin-positive vesicle attached to cilia (white arrowhead in A″). (B) Localization of serotonin-containing vesicles in SSCs. Cell boundaries marked by actin staining using phalloidin. Higher magnifications (left panels in B′-B‴) and orthogonal projection of *z*-stack slices (white dashed lines; right panels in B′-B‴) demonstrate serotonin-positive vesicles beneath, at, or above the apical cell membrane (B′-B‴, green arrowheads). (C) SEM of stage 32 tadpole displaying MCCs and SSCs. (C′) Higher magnification of two SSCs. Red arrowheads highlight detaching vesicles. Scale bars: 50 µm in A′; 10 µm in A″; 5 µm in B-B‴; 20 µm in C; 5 µm in C′.

Development (2014) doi:10.1242/dev.102343

relative position in the cell (supplementary material Fig. S1C). Apically localized vesicles were larger (with a diameter of up to 1 µm), compared with more basal ones, with a minimum diameter of 0.2 µm. Serotonin-positive vesicles were not detected at the basal pole of cells (supplementary material Fig. S1C). Taken together, SSCs appear a day later than MCCs and ISCs. They are characterized by small cell size and apical release of serotonin-containing vesicles, which clearly distinguishes them from goblet or ion-secreting cells (Dubaissi and Papalopulu, 2011; Hayes et al., 2007; Montorzi et al., 2000; Quigley et al., 2011). In the accompanying paper, Papalopulu and colleagues have independently identified and characterized a novel small secretory cell type in the embryonic skin of *Xenopus tropicalis* (Dubaissi et al., 2014). They used fluorescently labeled peanut agglutinin (PNA) to identify these cells. PNA and serotonin colocalized in secretory vesicles of the *Xenopus laevis* epidermis (supplementary material Fig. S1D), demonstrating that the identical cell type was identified in this study. Interestingly, PNA-positive signals were confined to more central vesicular regions, whereas serotonin was found in the periphery (supplementary material Fig. S1D′). Serotonin was thus not the only substance secreted by this novel epidermal cell type, which we name small secretory cell (SSC).

SSCs synthesize serotonin in the larval skin

Serotonin in SSCs could be derived from reuptake from the extracellular space or by *de novo* synthesis in SSCs itself. In order to investigate these options, we analyzed the expression of central components of serotonin biosynthesis in the epidermis of *Xenopus laevis*. During tadpole stages, mRNA expression of the serotonin reuptake transporter *slc6a4* was restricted to brain regions and not present in the epidermis (not shown), suggesting that SSCs do not use a reuptake mechanism. Next we analyzed mRNA distribution of the two vesicular monoamine transporters *slc18a1* and *slc18a2*, which are required for serotonin loading into vesicles. Expression of *slc18a2* mRNA was not detected in the tadpole. Signals were only seen during early cleavage stages (not shown). Transcription of *slc18a1*, however, was strongly induced at early neurula stages in the entire superficial layer of the epidermis, and was also observed in stage 24 tadpoles (supplementary material Fig. S2A). At later stages, *slc18a1* signals became weaker, with no obvious bias towards a specific cell type (supplementary material Fig. S2B). All types of epidermal cell (goblet cells, SSCs, ICSs and MCCs) should therefore, in principle, be competent to load serotonin into vesicles. The ubiquitous nature of *slc18a1* expression in the larval skin, however, prevents this gene from being used as a specific SSC marker.

Finally, we assessed the expression of two *tryptophan hydroxylase* genes, *tph1*and *tph2*, which encode the rate-limiting enzymes for serotonin synthesis. At early tadpole stages, *tph2* transcription was exclusively found in the hindbrain (supplementary material Fig. S2C), in agreement with the function of serotonin as a neurotransmitter. *tph1*, by contrast, showed a more complex expression pattern. Beginning at early tadpole stages, *tph1* mRNA was detected in the epiphysis, where the enzyme is required for melatonin synthesis (Fig. 2A) (Baker and Quay, 1969; Bellipanni et al., 2002). At stage 30, an additional neural expression site was detected in the floor plate, where staining was seen in individual cells and small cell clusters (Fig. 2A). Importantly, a punctate pattern was visible in the embryonic skin, first observed in early tadpoles (stage 23) and persisting to stage 42 (Fig. 2A). The dotted pattern indicated that SSCs might synthesize serotonin *de novo*. This notion was confirmed by colocalization of *tph1* mRNA with serotonin and PNA (Fig. 2B; supplementary material Fig. S2D,D′).

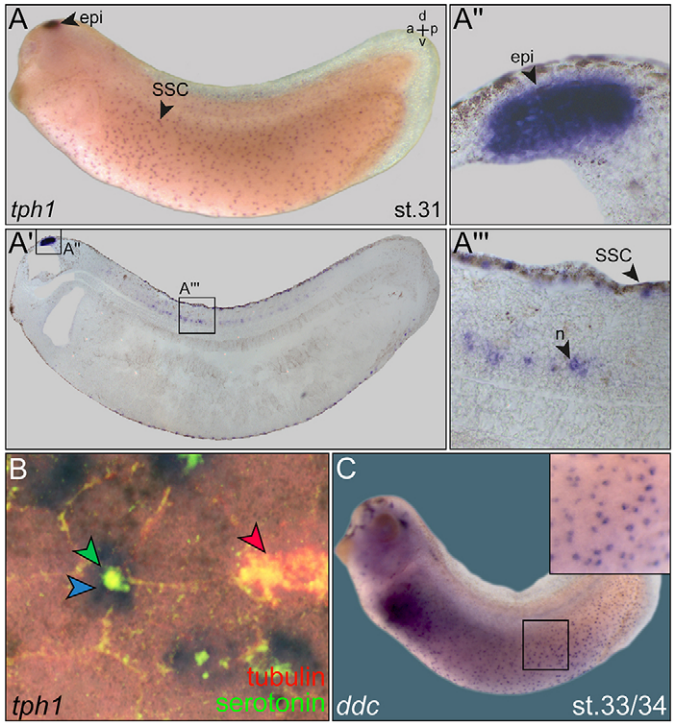

Fig. 2. SSCs express *tph1*. (A) Expression pattern of *tph1* mRNA at stage 31. Signals were detected in the brain and in a punctate pattern in the epidermis. A sagittal histological section (A′) demonstrated *tph1*expression in the epiphysis (A″) in SSCs and in a subset of neuronal cells (n) in the floor plate of the neural tube (A‴). (B) SSCs express *tph1* (blue arrowhead), as demonstrated by whole-mount *in situ* hybridization followed by IF for serotonin (green, green arrowhead) and cilia (acetylated-α-tubulin, red, red arrowhead). (C) Punctate expression pattern of *aromatic-L-amino-acid decarboxylase* (*DOPA-decarboxylase*; *ddc*) in the embryonic skin. Inset shows close-up. Embryos are shown in lateral views. a, anterior; d, dorsal; epi, epiphysis; l, left; r, right.

Finally, *aromatic-L-amino-acid* or *DOPA-decarboxylase* (*ddc*), which catalyzes the final step in serotonin biosynthesis, was expressed in a similar pattern (Fig. 2C). Together these marker analyses strongly suggest that SSCs synthesize serotonin *de novo* in the larval skin.

Serotonin regulates cilia-driven fluid flow in the larval skin

Serotonin synthesis in the epidermis gave us the opportunity to test directly the functional relevance of serotonin signaling in the frog tadpole MCE. To this end, we used a selective and irreversible pharmacological inhibitor of TPH function, *para*-chlorophenylalanine (PCPA), which depletes serotonin from cells (Engelman et al., 1967). Tadpoles were treated with PCPA from stage 25 onwards and analyzed for serotonin localization at stage 32 (Fig. 3A). Co-staining with phalloidin was used to monitor epidermal cell morphology. Untreated control embryos showed vesicular localization of serotonin, whereas no signals were detected in PCPA-treated specimens (Fig. 3C,C′). The serotonin-depleted epidermis appeared morphologically unaltered, as judged by the integrity of the actin cytoskeleton as well as by the number and length of MCC cilia (Fig. 3A,C′; not shown). In addition, *tph1* expression was unchanged in PCPA-treated specimens, demonstrating that cell fate of serotonin-secreting cells was not affected (Fig. 3D,D′). Close examination of phalloidin staining, however, revealed small membrane areas at positions were SSCs

Development (2014) doi:10.1242/dev.102343

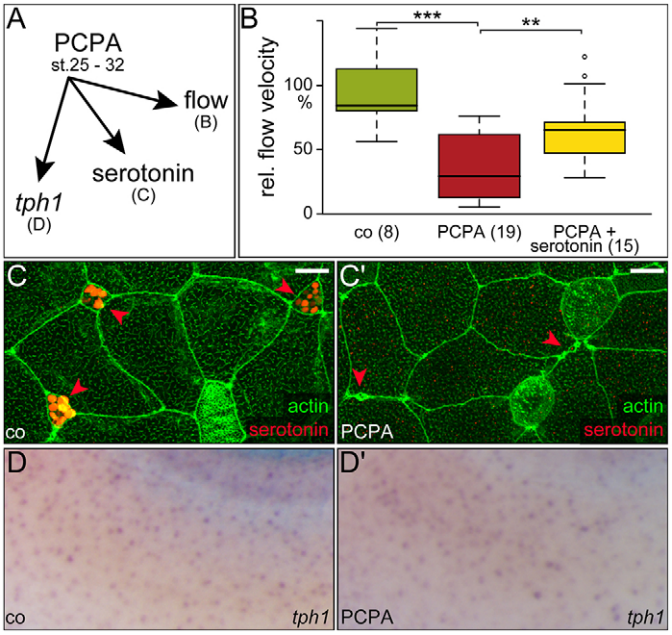

Fig. 3. Inhibition of serotonin synthesis impairs cilia-driven flow. (A) Experimental setup. Embryos were incubated with TPH inhibitor p-chloro-phenylalanin (PCPA) from stage 25-32, followed by assessment of flow (B), serotonin localization (C) and *tph1* expression (D). (B) Reduction of flow velocity in PCPA-treated specimen was partially rescued by co-culture with exogenously applied serotonin. Flow was analyzed by data processing from time-lapse movies following the addition of fluorescent beads to the medium. The mean velocity in control embryo was set to 100%. (C) Absence of serotonin staining (red arrowheads) upon PCPA incubation (C′). (D) Unaltered *tph1* expression following PCPA treatment (D′).

would normally be found (Fig. 3C′), indicating that apical expansion of SSCs into the outer epithelial layer was disturbed.

Serotonin has previously been demonstrated to regulate CBF in a number of systems (Doran et al., 2004; Nguyen et al., 2001; Wada et al., 1997). To test whether loss of serotonin synthesis affected cilia-driven fluid flow in the larval skin, flow velocity was analyzed in PCPA-treated specimens. Fluorescent beads were added to embryos and bead movements were tracked by time-lapse videography. The mean velocity of untreated control tadpoles was set to 100% for each experiment in order to account for variabilities between embryo batches (cf. Materials and Methods). PCPA treatment reduced cilia-driven flow by about two-thirds ($P<0.001$; Fig. 3B; supplementary material Movie 1). Importantly, incubation with PCPA and serotonin rescued flow velocity to 60% of the value in untreated controls, demonstrating the specificity of our observation ($P<0.01$; Fig. 3B). From these data, we conclude that serotonin modulates the velocity of cilia-dependent flow of extracellular mucus at the *Xenopus* skin.

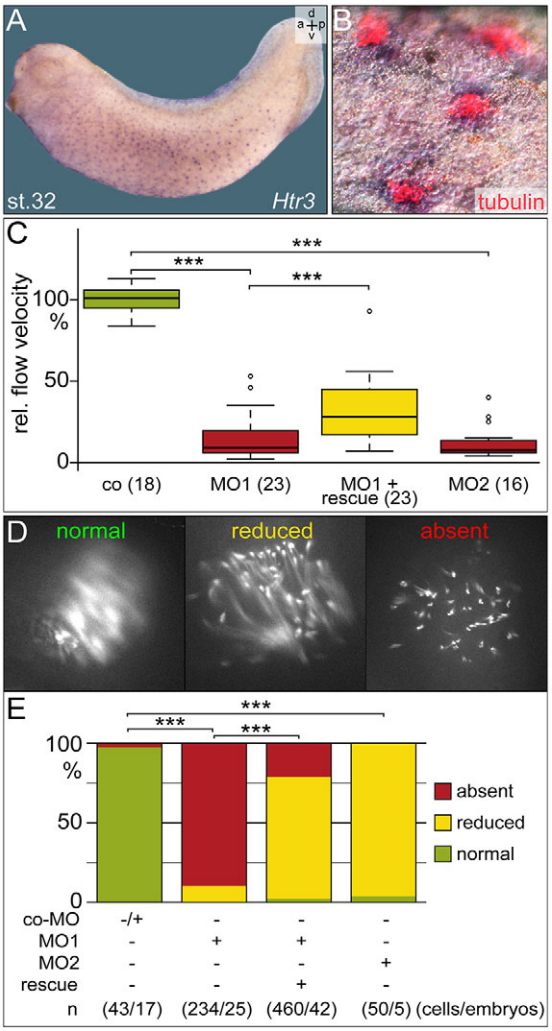

Fig. 4. The serotonin receptor *Htr3* controls cilia motility in the tadpole epidermis. (A,B) Punctate serotonin receptor *Htr3* mRNA expression in stage 31 epidermis (A) colocalizes to MCCs, demonstrated by double-staining with anti-acetylated tubulin antibody (B). (C) Reduction of flow velocity in *Htr3* morphants. Knockdown of *Htr3* by MO1 and MO2 reduced cilia-driven flow velocity compared with control specimens (co). Velocity was partially rescued by co-injection of a mutated *Htr3* mRNA not targeted by MO1. Flow was analyzed by adding fluorescent beads to the medium and data processing of time-lapse movies. The mean velocity in control embryo was set to 100%. (D,E) Cilia motility in the epidermis of co-MO and *Htr3*-MO injected specimens. Cilia were visualized by co-injection of mRFP mRNA. (D) Maximum *z*-projections (stacks of 450 frames) from time-lapse movies (5-second duration). Blurring indicates motion, acuity lack thereof. (E) Quantification of results. Note rescue of ciliary motility by co-injection of mutated *Htr3* mRNA or DNA construct, which is not targeted by *Htr3*-MO. a, anterior; d, dorsal; l, left; r, right.

Regulation of ciliary beat frequency through serotonin receptor *Htr3*

Next we asked how serotonin signaling impacts on cilia-driven flow. Two scenarios could be envisaged: on the one hand, serotonin signal transduction might regulate the molecular composition of the released mucus. In this case, loss of serotonin would result in the secretion of a more viscous mucus, impeding cilia-driven flow indirectly. On the other hand, serotonin signaling could modulate CBF in a positive manner in MCCs, in much the same way as has been shown for ependymal or tracheal cilia in rat and mouse (König et al., 2009; Nguyen et al., 2001). In both scenarios, effects should be receptor dependent. To identify candidate receptors we analyzed nine *bona fide Xenopus* serotonin receptors (*Htr1a*, *1e/f*, *2a*, *2b*, *2c*, *3*, *4*, *5a*, *6* and *7*) for epidermal expression patterns using whole-mount *in situ* hybridization. Of these, only the type 3 receptor *Htr3*, which encodes a ligand gated ion channel, showed positive signals in the epidermis (Fig. 4A). A regular punctate pattern was detected in the embryonic skin from stage 21 onwards (Fig. 4A). Double staining of *Htr3* mRNA and cilia revealed *Htr3* expression in multiciliated cells (Fig. 4B).

Development (2014) doi:10.1242/dev.102343

We recently demonstrated a role for *Htr3* in Wnt/β-catenin dependent expression of *foxj1* during blastula/gastrula stages (Beyer et al., 2012). As *foxj1* induces motile cilia in epidermal MCCs as well (Stubbs et al., 2008), we wondered whether *Htr3* might be required for *foxj1* expression in the skin. Two previously characterized nonoverlapping antisense morpholino oligonucleotides (*Htr3*-MO1/2) were used to perform loss-of-function experiments. MOs targeted the translational start site (MO1) or the 5′ UTR (MO2; Beyer et al., 2012). MO-specificity was tested by injection of an eGFP construct, which contained MO1- and MO2-binding site in its 5′ UTR. Fluorescence was lost upon co-injection of MO1 or MO2 (supplementary material Fig. S3A-C). In a first set of experiments, we applied MO1 unilaterally to the epidermis by injecting animal hemispheres of ventral blastomeres at the four- to eight-cell stage. When tadpoles reached stage 16, *foxj1* expression in the skin was assessed comparing injected and uninjected sides. No reduction of *foxj1* expression was detected in morphants (supplementary material Fig. S3D,E).

Impaired cilia-driven hovering of embryos, however, was observed when embryos were placed on the injected side at stage 32 (data not shown). These effects were seen following MO1 or MO2 injection, but not using a control MO (coMo). To analyze the underlying mucus flow in a quantitative manner, we compared flow velocities of untreated controls and morphants by imaging of fluorescent particle movements. Flow velocities were greatly reduced by both MOs, to ~20% or less of the control values (P<0.001; Fig. 4C; supplementary material Movie 2). This effect was specific as co-injection of MO1 with a mutated *Htr3* mRNA, in which the MO1 binding site was altered (Beyer et al., 2012), partially rescued flow velocity (P<0.001; Fig. 4C). To exclude the possibility that *Htr3* was involved in ciliogenesis downstream of *foxj1*, we analyzed MO1 morphants and control specimens for MCC density, ciliation and cilia length. Morphants showed no signs of overt ciliogenesis defects (supplementary material Fig. S3F,G), suggesting that altered ciliary beating was responsible for the observed flow defects. To directly test an effect of *Htr3* loss-of-function on CBF, we visualized ciliary beating by co-injection of membrane RFP. This analysis revealed wild-type motility in coMO-injected specimens and reduced or absent ciliary motility in MO1 or MO2 morphants, with MO1-injections resulting in more pronounced effects (Fig. 4C,D; supplementary material Movie 3). Because of its higher efficiency, we confirmed MO specificity for MO1. The *Htr3* rescue construct, when co-injected with MO1 as mRNA or DNA expression construct, rescued cilia motility, further demonstrating the specificity of MO effects (P<0.001; Fig. 4E). Together, these functional experiments demonstrate that serotonin, secreted from SSCs and mediated through receptor type 3, is required for ciliary motility of MCCs and thus for the regulation of mucus transport across the embryonic tadpole skin.

DISCUSSION

The identification and functional analysis of serotonin-secreting cells in the tadpole skin of *Xenopus laevis* adds a novel and highly relevant component to this important animal model system of human MCE. Figure 5 summarizes our current interpretation of the developmental function of the tadpole MCE. MCCs and ISCs arise from the deep ectodermal layer that contains a pool of precursor cells (Dubaissi and Papalopulu, 2011; Quigley et al., 2011; Stubbs et al., 2006), which are specified much earlier than SSCs (neurula versus early tadpole stages, respectively). The accompanying paper by Dubaissi and colleagues, however, shows that SSCs intercalate into the superficial epidermal cell layer as well, which is paralleled

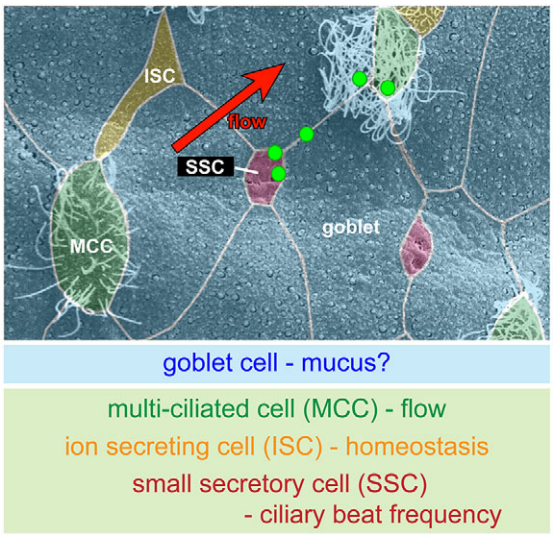

Fig. 5. Regulation and function of cell types at the *Xenopus* tadpole epidermis: a model. SSCs constitute a novel cell type in the mucociliary epithelium of the *Xenopus laevis* tadpole skin. Serotonin is released in vesicles (green circles) and transported to MCCs by flow. Following release, serotonin modulates ciliary beat frequency via serotonin receptor 5-HT3.

by the appearance of multiple serotonin containing vesicle-like structures (Dubaissi et al., 2014). During further development, vesicles progressively localize to the apical surface and get released in due course. Following inhibition of serotonin synthesis, vesicles were mostly lost (cf. Fig. 2B′), suggesting that serotonin either represents a major component of vesicles or serotonin is required for vesicle loading with other substances. If and how this observation is linked to the inability of serotonin-deprived SSCs to fully expand their apical surface area remains elusive. Serotonin-loaded vesicles might produce some sort of mechanical force during apical translocation, which pushes neighboring cells apart. Alternatively, an autocrine feedback mechanism might govern the emergence of SSCs. Unraveling the molecular mechanism of vesicle loading, transport and secretion will serve to solve this issue.

The observed secretion mechanism, i.e. by shedding of large serotonin-containing vesicles, was unexpected and has not been described in vertebrates before. Typically, serotonin vesicles destined for secretion are exocytosed through plasma membrane fusion and release of serotonin into the extracellular space. In airway epithelia, Clara cells use both exocytosis and apocrine secretion, depending on environmental conditions (Reynolds and Malkinson, 2010). SSCs might therefore use exocytosis for serotonin secretion as well. Future studies using markers for exosomal release via multivesicular bodies or apocrine secretion through plasma membrane blebs should help to identify the underlying mechanism. Large serotonin-positive granules have previously been identified in the mucus of the ciliated foot epithelium of the pond snail *Lymnaea stagnalis appressa* (Longley and Peterman, 2012), in which CBF regulation by serotonin was demonstrated as well, suggesting that this type of serotonin dispersal could be more widespread.

The occasional observation of vesicles attached to cilia might reflect a snapshot of a scenario in which vesicles are transported by flow and disintegrate through ciliary beating (Fig. 5). Such a mechanism would result in a locally high concentration of serotonin near MCCs, where receptors could enhance CBF. A likely mechanism has been previously proposed during left-right axis determination in the mouse embryo. Nodal vesicular parcels (NVPs)

Development (2014) doi:10.1242/dev.102343

were found at the posterior notochord/'node', where cilia-driven flow breaks the bilateral symmetry of the mouse embryo. It has been suggested that NVPs are transported through flow and burst to release signaling molecules, which would initiate asymmetric signaling (Hirokawa et al., 2006). *In vivo* labeling of serotonin-containing vesicles and live imaging should allow detection of such a mechanism if it existed in the larval MCE. As well as this unresolved question, our data demonstrate that serotonin regulates CBF in the frog embryo, consistent with reports throughout the animal kingdom.

The finding that a receptor type 3 (5-HT3) regulates CBF was surprising. In rat ependyma, 5-HT2 was shown to mediate the serotonin signals to ciliated cells (Nguyen et al., 2001), whereas 5-HT1 or 5-HT7 were identified in mollusks (Doran et al., 2004; Longley and Peterman, 2012). Most of the 20 or so serotonin receptor genes, which are grouped in seven families based on downstream effectors, encode seven-span transmembrane G-protein coupled receptors. The sole exception are type 3 receptors, which code for ligand-gated ion channels, with a prime selectivity for calcium (Barnes and Sharp, 1999). Although 5-HT3 has not previously been shown to be involved in CBF regulation, a link of this receptor class to cilia has been documented. The most abundant receptor gene expressed in cultured rat ependyma cells was found to be *Htr3* (Verleysdonk et al., 2005). Human primary alveolar epithelial cells and lung cell lines also express *HTR3* mRNA (Bayer et al., 2007), indicating that 5-HT3 might act on CBF in other ciliated tissues as well. Importantly, cytoplasmic Ca^{2+} was shown to be the major regulator of CBF in many systems (Schmid and Salathe, 2011). An increase in Ca^{2+}-levels in ciliated cells was correlated with elevated CBF in MCE (Braiman and Priel, 2008). In rat ependymal cells, serotonin-induced CBF stimulation was dependent on Ca^{2+}-influx and elevated Ca^{2+}-levels in ciliated cells (Nguyen et al., 2001). The Ca^{2+}-channel 5-HT3 is particularly suited to regulate the frequency of ciliary beating directly by an increase of Ca^{2+}-levels upon serotonin binding. Serotonin-dependent Ca^{2+}-influx has been demonstrated in human primary alveolar epithelial cells and various lung cell lines as well (Bayer et al., 2007), although CBF was not analyzed in this study. Taken together, regulation of CBF through serotonin/5-HT3-mediated Ca^{2+}-influx might not be restricted to the frog skin MCE but represent a widespread mechanism of ciliary beat control.

The source of serotonin regulating CBF also seems variable, particularly with respect to the cellular identity of synthesizing cells. In frog, source (SSCs) and target (MCCs) are juxtaposed in the same epithelium, indicating a short range dispersal of serotonin. In brain ependyma, a dense supra-ependymal meshwork of free serotonergic axons was identified as source of serotonin, which was found directly attached to the ventricular cell layer (Del Bigio, 2009). CBF regulation by synaptic neuronal innervation of ciliated cells was shown in snail embryos (Kuang et al., 2002; Longley and Peterman, 2012; Syed and Winlow, 1989). Subepithelial mast cells or blood platelets were proposed as a source of serotonin in the mouse trachea (König et al., 2009). In the mammalian tracheo-bronchial epithelium, single serotonin-producing cells (neuroendocrine cells) or cell clusters (neuroendocrine bodies) were described (Cutz et al., 2013; Linnoila, 2006; Van Lommel, 2001). Although serotonin secretion into the airway lumen has not been demonstrated, serotonin released from neuroendocrine cells might influence ciliary beating in neighboring ciliated cells. Despite tissue and species differences, we like to suggest a common chemosensory function of serotonin-secreting cells. Airway neuroendocrine cells release serotonin upon hypoxia (Fu et al., 2002; Linnoila, 2006). Serotonergic neurons in the Raphe nuclei of the brain stem have been implicated in respiratory chemosensation as well (Corcoran et al., 2009). Interestingly, a subset of Raphe nuclei project axons to the ependymal epithelium. In snail embryos, hypoxia was shown to be sensed by serotonergic neurons, resulting in an enhanced CBF upon serotonin signaling (Goldberg et al., 2011; Kuang et al., 2002). Based on these reports it seems conceivable that serotonin-secreting cells in *Xenopus laevis* might have a sensory function as well.

The accompanying manuscript by Dubaissi et al. describes SSCs in the epidermis of *Xenopus tropicalis* and demonstrates their specification by the forkhead transcription factor *foxa1* (Dubaissi et al., 2014). The colocalization of peanut agglutinin and serotonin in both species clearly demonstrates that the identical cell type was characterized in these studies. Additional common characteristics comprise the presence of large vesicles as well as embryonic death upon serotonin depletion (not shown) or *foxa1* knockdown (Dubaissi et al., 2014). Intriguingly, *Xenopus tropicalis* SSCs release mucus-like substances, physically protecting the epidermis against bacterial infections (Dubaissi et al., 2014). Thus, general functions of MCE, mucus production and secretion as well as maintenance of cilia-driven flow velocity (i.e. CBF regulation via serotonin secretion) are combined in a single epidermal cell type. As serotonin has been shown to stimulate mucus secretion in the gastrointestinal tract of mammals (Hansen and Witte, 2008), serotonin could also influence mucus secretion in the larval skin of *Xenopus*, either acting on SSCs in an autocrine loop or in a paracrine manner affecting goblet cells. A dual function of serotonin on ciliary beating and mucus release has indeed been experimentally demonstrated in the MCE of the adult frog palatine mucosa (Maruyama et al., 1984). It remains to be seen whether such a serotonin activity is present in the *Xenopus* epidermis as well.

The present study and accompanying study (Dubaissi et al., 2014) underscore the relevance of the embryonic *Xenopus* skin as a model to analyze the biology of mucociliary epithelia. The simplicity and accessibility of the system allows in-depth analyses at multiple levels, the identification of the molecular mechanisms of the secretion mechanism, of vesicle contents and of environmental factors acting on vesicle release. Future investigation of a potential sensory regulatory circuit in the *Xenopus* embryonic skin, involving SSCs, serotonin release, regulation of CBF and mucus velocity as well as environmental cues will impact on our understanding of other mucociliary epithelia, including the human airway epithelium.

MATERIALS AND METHODS

RNA *in situ* hybridization and scanning electron microscopy (SEM)

Embryos were fixed in MEMFA for 2 hours and processed following standard protocols. Digoxigenin-labeled (Roche) RNA probes were prepared from linearized plasmids using SP6 or T7 RNA polymerase (Promega). *In situ* hybridization was according to Belo et al. (Belo et al., 1997). Sequences of probes used correspond to: *tph1* (L20679; Green et al., 1995), *tph2* (KF192076), *Htr3* (BC044101; Beyer et al., 2012), *slc18a1* (coding region of BC041717) and *ddc* (762 bp fragment of NM_001110741.1). SEM analysis was performed as described (Sulik et al., 1994).

Motility of epidermal cilia bundles

Motility of epidermal cilia bundles was analyzed by time-lapse videography (90 fps, 5 seconds). Embryos were unilaterally injected into animal-ventral blastomeres at the four- to eight-cell stage with 800 pg *mRFP*-mRNA and 2 pmol co-MO, 1.7-2 pmol *Htr3*-MO1 or 1.7 pmol *Htr3*-MO2. In rescue experiments, 240 pg *Htr3* mRNA and/or 12 pg DNA lacking the MO1 binding site were co-injected. Sequence of MO and design of rescue construct was as described in Beyer et al. (Beyer et al., 2012). Motility of cilia bundles was classified into three categories: normal motility, reduced

motility and immobility of cilia (cf. Fig. 4D; supplementary material Movie 2). Significances were calculated by comparing immotile cilia with normal and reduced motility using Pearson's χ^2 test (Bonferroni corrected; Statistica 6.1 – StatSoft).

Immunofluorescence (IF)

IF was performed on whole-mount embryos fixed in 4% PFA for 1-2 hours at room temperature. Embryos were processed according to standard procedures (Sive et al., 2000). Primary antibodies: mouse monoclonal antibody against acetylated alpha tubulin (1:700; T6793, Sigma): rabbit polyclonal anti-serotonin antibody (1:500; AB938, Merck). Secondary antibodies: Cy2- or Cy3-conjugated polyclonal rabbit or sheep anti-mouse antibodies (Jackson ImmunoResearch or Sigma; both 1:250); Alexa Fluor 488- or 555-conjugated donkey or goat anti-rabbit antibodies (both 1:250; Invitrogen). Actin staining was performed by 30-60 minute incubation with Alexa Fluor 488 Phalloidin (1:40; Invitrogen). Fluorescently labeled peanut agglutinin (PNA Alexa Fluor 568; Life Technologies) was incubated overnight at 4°C and used in 1:1000 dilution of a 1 mg/ml stock solution. ImageJ was used for *z*-stack analysis (Schindelin et al., 2012).

Pharmacological treatments and determination of fluid flow velocity

PCPA (Sigma) and serotonin (Sigma) solutions of 80-150 µM and 1 mM, respectively, were prepared in 0.1×MBSH directly before incubation. PCPA incubations and co-incubations with serotonin were initiated at stage 25 and performed at room temperature. At stage 32-34, embryos were fixed for whole-mount *in situ* hybridization, IF or imaging. Flow was also analyzed in embryos injected unilaterally with *Htr3* MO1 (1-1.3 pmol/embryo) and MO2 (2-2.5 pmol/embryo) into the ventral animal blastomeres at the four- to eight-cell stage. Rescue of flow was achieved by co-injection of 400 pg of mutated *Htr3* mRNA. FITC-conjugated latex beads (0.5 µm; Life Technologies) were diluted to 0.04% in 0.1×MBSH containing benzocaine (Sigma) in order to anesthetize embryos. Time-lapse imaging was performed at a rate of 28.5 frames per second for 10 seconds in a sealed flow chamber using 10×magnification on a Zeiss microscope. Time-lapse movies were processed in ImageJ and a sector with laminar flow was chosen for automated analysis using the ImageJ plugin ParticleTracker (Sbalzarini and Koumoutsakos, 2005). As velocities of untreated controls differed between embryo batches (~60-300 µm/s mean velocity; data not shown), the mean velocity of controls was set to 100% of relative flow velocity. For calculation of flow and statistical analysis of differences in relative flow velocity, Rayleigh test of uniformity and Wilcoxon sum of ranks (Mann–Whitney) tests were used (R Development Core Team, 2005).

Experimental animals

Handling and experimental manipulations of *Xenopus laevis* were according to German laws and regulations (§6, article 1, sentence 2, nr. 4 of the animal protection act) and approved by the Regional Government Stuttgart, Germany (Vorhaben A 365/10 ZO 'Molekulare Embryologie').

Acknowledgements

We thank Stine Mencl, Eva-Maria Sawert and Matthias Tisler for help with some of the experiments; Michael Levin, Chris Kintner and John Wallingford for plasmids and antibodies; Werner Amselgruber for help with SEM analysis; and Nancy Papalopulu for sharing data and reagents prior to publication.

Competing interests

The authors declare no competing financial interests.

Author contributions

P.W., S.B., T.T., P.V. and T.B. performed experiments. Experiments were conceived and designed by P.W., M.B. and A.S. The manuscript was written by A.S. and edited by M.B., P.W., T.T., E.D. and P.V.

Funding

Work in the Blum lab was supported by a grant from the Deutsche Forschungsgemeinschaft [BL-285/9]. P.V., T.T., T.B. and P.W. were recipients of PhD fellowships from the Landesgraduiertenförderung Baden-Württemberg.

Supplementary material

Supplementary material available online at
http://dev.biologists.org/lookup/suppl/doi:10.1242/dev.102343/-/DC1

References

Albee, A. J. and Dutcher, S. K. (2012). *Cilia and Human Disease*. Chichester, UK: John Wiley & Sons Ltd.

Amireault, P., Sibon, D. and Côté, F. (2013). Life without peripheral serotonin: insights from tryptophan hydroxylase 1 knockout mice reveal the existence of paracrine/autocrine serotonergic networks. *ACS Chem Neurosci* **4**, 64-71.

Baker, P. C. and Quay, W. B. (1969). 5-hydroxytryptamine metabolism in early embryogenesis, and the development of brain and retinal tissues. A review. *Brain Res.* **12**, 273-295.

Barnes, N. M. and Sharp, T. (1999). A review of central 5-HT receptors and their function. *Neuropharmacology* **38**, 1083-1152.

Bayer, H., Müller, T., Myrtek, D., Sorichter, S., Ziegenhagen, M., Norgauer, J., Zissel, G. and Idzko, M. (2007). Serotoninergic receptors on human airway epithelial cells. *Am. J. Respir. Cell Mol. Biol.* **36**, 85-93.

Bellipanni, G., Rink, E. and Bally-Cuif, L. (2002). Cloning of two tryptophan hydroxylase genes expressed in the diencephalon of the developing zebrafish brain. *Mech. Dev.* **119** Suppl. 1, S215-S220.

Belo, J. A., Bouwmeester, T., Leyns, L., Kertesz, N., Gallo, M., Follettie, M. and De Robertis, E. M. (1997). Cerberus-like is a secreted factor with neutralizing activity expressed in the anterior primitive endoderm of the mouse gastrula. *Mech. Dev.* **68**, 45-57.

Berger, M., Gray, J. A. and Roth, B. L. (2009). The expanded biology of serotonin. *Annu. Rev. Med.* **60**, 355-366.

Beyer, T., Danilchik, M., Thumberger, T., Vick, P., Tisler, M., Schneider, I., Bogusch, S., Andre, P., Ulmer, B., Walentek, P. et al. (2012). Serotonin signaling is required for Wnt-dependent GRP specification and leftward flow in Xenopus. *Curr. Biol.* **22**, 33-39.

Brailov, I., Bancila, M., Brisorgueil, M. J., Miquel, M. C., Hamon, M. and Vergé, D. (2000). Localization of 5-HT(6) receptors at the plasma membrane of neuronal cilia in the rat brain. *Brain Res.* **872**, 271-275.

Braiman, A. and Priel, Z. (2008). Efficient mucociliary transport relies on efficient regulation of ciliary beating. *Respir. Physiol. Neurobiol.* **163**, 202-207.

Castrodad, F. A., Renaud, F. L., Ortiz, J. and Phillips, D. M. (1988). Biogenic amines stimulate regeneration of cilia in Tetrahymena thermophila. *J. Protozool.* **35**, 260-264.

Corcoran, A. E., Hodges, M. R., Wu, Y., Wang, W., Wylie, C. J., Deneris, E. S. and Richerson, G. B. (2009). Medullary serotonin neurons and central CO2 chemoreception. *Respir. Physiol. Neurobiol.* **168**, 49-58.

Cowan, M. J., Gladwin, M. T. and Shelhamer, J. H. (2001). Disorders of ciliary motility. *Am. J. Med. Sci.* **321**, 3-10.

Cutz, E., Pan, J., Yeger, H., Domnik, N. J. and Fisher, J. T. (2013). Recent advances and contraversies on the role of pulmonary neuroepithelial bodies as airway sensors. *Semin. Cell Dev. Biol.* **24**, 40-50.

Del Bigio, M. R. (2009). Ependymal cells: biology and pathology. *Acta Neuropathol.* **119**, 55-73.

Doran, S. A., Koss, R., Tran, C. H., Christopher, K. J., Gallin, W. J. and Goldberg, J. I. (2004). Effect of serotonin on ciliary beating and intracellular calcium concentration in identified populations of embryonic ciliary cells. *J. Exp. Biol.* **207**, 1415-1429.

Dubaissi, E. and Papalopulu, N. (2011). Embryonic frog epidermis: a model for the study of cell-cell interactions in the development of mucociliary disease. *Dis. Model. Mech.* **4**, 179-192.

Dubaissi, E., Rousseau, K., Lea, R., Soto, X., Nardeosingh, S., Schweickert, A., Amaya, E., Thornton, D. J. and Papalopulu, N. (2014). A secretory cell type develops alongside multiciliated cells, ionocytes and goblet cells, and provides a protective, anti-infective function in the frog embryonic mucociliary epidermis. *Development* **141**, 1513-1524.

Ducy, P. and Karsenty, G. (2010). The two faces of serotonin in bone biology. *J. Cell Biol.* **191**, 7-13.

Engelman, K., Lovenberg, W. and Sjoerdsma, A. (1967). Inhibition of serotonin synthesis by para-chlorophenylalanine in patients with the carcinoid syndrome. *N. Engl. J. Med.* **277**, 1103-1108.

Fu, X. W., Nurse, C. A., Wong, V. and Cutz, E. (2002). Hypoxia-induced secretion of serotonin from intact pulmonary neuroepithelial bodies in neonatal rabbit. *J. Physiol.* **539**, 503-510.

Fukumoto, T., Kema, I. P. and Levin, M. (2005). Serotonin signaling is a very early step in patterning of the left-right axis in chick and frog embryos. *Curr. Biol.* **15**, 794-803.

Goldberg, J. I., Rich, D. R., Muruganathan, S. P., Liu, M. B., Pon, J. R., Tam, R., Diefenbach, T. J. and Kuang, S. (2011). Identification and evolutionary implications of neurotransmitter-ciliary interactions underlying the behavioral response to hypoxia in Lymnaea stagnalis embryos. *J. Exp. Biol.* **214**, 2660-2670.

Green, C. B., Cahill, G. M. and Besharse, J. C. (1995). Regulation of tryptophan hydroxylase expression by a retinal circadian oscillator in vitro. *Brain Res.* **677**, 283-290.

Gutknecht, L., Kriegebaum, C., Waider, J., Schmitt, A. and Lesch, K.-P. (2009). Spatio-temporal expression of tryptophan hydroxylase isoforms in murine and human brain: convergent data from Tph2 knockout mice. *Eur. Neuropsychopharmacol.* **19**, 266-282.

Hansen, M. B. and Witte, A.-B. (2008). The role of serotonin in intestinal luminal sensing and secretion. *Acta Physiol. (Oxf.)* **193**, 311-323.

Hayes, J. M., Kim, S. K., Abitua, P. B., Park, T. J., Herrington, E. R., Kitayama, A., Grow, M. W., Ueno, N. and Wallingford, J. B. (2007). Identification of novel ciliogenesis factors using a new in vivo model for mucociliary epithelial development. *Dev. Biol.* **312**, 115-130.
Hirokawa, N., Tanaka, Y., Okada, Y. and Takeda, S. (2006). Nodal flow and the generation of left-right asymmetry. *Cell* **125**, 33-45.
König, P., Krain, B., Krasteva, G. and Kummer, W. (2009). Serotonin increases cilia-driven particle transport via an acetylcholine-independent pathway in the mouse trachea. *PLoS ONE* **4**, e4938.
Kuang, S., Doran, S. A., Wilson, R. J. A., Goss, G. G. and Goldberg, J. I. (2002). Serotonergic sensory-motor neurons mediate a behavioral response to hypoxia in pond snail embryos. *J. Neurobiol.* **52**, 73-83.
Linnoila, R. I. (2006). Functional facets of the pulmonary neuroendocrine system. *Lab. Invest.* **86**, 425-444.
Livraghi, A. and Randell, S. H. (2007). Cystic fibrosis and other respiratory diseases of impaired mucus clearance. *Toxicol. Pathol.* **35**, 116-129.
Longley, R. D. and Peterman, M. (2013). Neuronal control of pedal sole cilia in the pond snail Lymnaea stagnalis appressa. *J. Comp. Physiol. A*. 199, 71-86.PubMed
Maruyama, I., Inagaki, M. and Momose, K. (1984). The role of serotonin in mucociliary transport system in the ciliated epithelium of frog palatine mucosa. *Eur. J. Pharmacol.* **106**, 499-506.
Mawe, G. M., Coates, M. D. and Moses, P. L. (2006). Review article: intestinal serotonin signalling in irritable bowel syndrome. *Aliment. Pharmacol. Ther.* **23**, 1067-1076.
Montorzi, M., Burgos, M. H. and Falchuk, K. H. (2000). Xenopus laevis embryo development: arrest of epidermal cell differentiation by the chelating agent 1,10-phenanthroline. *Mol. Reprod. Dev.* **55**, 75-82.
Nguyen, T., Chin, W.-C., O'Brien, J. A., Verdugo, P. and Berger, A. J. (2001). Intracellular pathways regulating ciliary beating of rat brain ependymal cells. *J. Physiol.* **531**, 131-140.
Nickells, R. W., Cavey, M. J. and Browder, L. W. (1988). The effects of heat shock on the morphology and protein synthesis of the epidermis of Xenopus laevis larvae. *J. Cell Biol.* **106**, 905-914.
Quigley, I. K., Stubbs, J. L. and Kintner, C. (2011). Specification of ion transport cells in the Xenopus larval skin. *Development* **138**, 705-714.
Reynolds, S. D. and Malkinson, A. M. (2010). Clara cell: progenitor for the bronchiolar epithelium. *Int. J. Biochem. Cell Biol.* **42**, 1-4.
R Development Core Team (2005). *R: A Language and Environment for Statistical Computing*. R Foundation for Statistical Computing, Vienna, Austria.
Rubin, B. K. (2007). Mucus structure and properties in cystic fibrosis. *Paediatr. Respir. Rev.* **8**, 4-7.
Sawamoto, K., Wichterle, H., Gonzalez-Perez, O., Cholfin, J. A., Yamada, M., Spassky, N., Murcia, N. S., Garcia-Verdugo, J. M., Marin, O., Rubenstein, J. L. R. et al. (2006). New neurons follow the flow of cerebrospinal fluid in the adult brain. *Science* **311**, 629-632.
Sbalzarini, I. F. and Koumoutsakos, P. (2005). Feature point tracking and trajectory analysis for video imaging in cell biology. *J. Struct. Biol.* **151**, 182-195.
Schindelin, J., Arganda-Carreras, I., Frise, E., Kaynig, V., Longair, M., Pietzsch, T., Preibisch, S., Rueden, C., Saalfeld, S., Schmid, B. et al. (2012). Fiji: an open-source platform for biological-image analysis. *Nat. Methods* **9**, 676-682.
Schmid, A. and Salathe, M. (2011). Ciliary beat co-ordination by calcium. *Biol. Cell* **103**, 159-169.
Sive, H. L., Grainger, R. M. and Harland, R. M. (2000). *Early Development of Xenopus Laevis: A Laboratory Manual*. Cold Spring Harbor, NY: Cold Spring Harbor Laboratory Press.
Stubbs, J. L., Davidson, L., Keller, R. and Kintner, C. (2006). Radial intercalation of ciliated cells during Xenopus skin development. *Development* **133**, 2507-2515.
Stubbs, J. L., Oishi, I., Izpisúa Belmonte, J. C. and Kintner, C. (2008). The forkhead protein Foxj1 specifies node-like cilia in Xenopus and zebrafish embryos. *Nat. Genet.* **40**, 1454-1460.
Stubbs, J. L., Vladar, E. K., Axelrod, J. D. and Kintner, C. (2012). Multicilin promotes centriole assembly and ciliogenesis during multiciliate cell differentiation. *Nat. Cell Biol.* **14**, 140-147.
Sulik, K., Dehart, D. B., Iangaki, T., Carson, J. L., Vrablic, T., Gesteland, K. and Schoenwolf, G. C. (1994). Morphogenesis of the murine node and notochordal plate. *Dev. Dyn.* **201**, 260-278.
Syed, N. I. and Winlow, W. (1989). Morphology and electrophysiology of neurons innervating the ciliated locomotor epithelium in Lymnaea stagnalis (L.). *Comp. Biochem. Physiol.* **93**, 633-644.
Van Lommel, A. (2001). Pulmonary neuroendocrine cells (PNEC) and neuroepithelial bodies (NEB): chemoreceptors and regulators of lung development. *Paediatr. Respir. Rev.* **2**, 171-176.
Verleysdonk, S., Kistner, S., Pfeiffer-Guglielmi, B., Wellard, J., Lupescu, A., Laske, J., Lang, F., Rapp, M. and Hamprecht, B. (2005). Glycogen metabolism in rat ependymal primary cultures: regulation by serotonin. *Brain Res.* **1060**, 89-99.
Wada, Y., Mogami, Y. and Baba, S. (1997). Modification of ciliary beating in sea urchin larvae induced by neurotransmitters: beat-plane rotation and control of frequency fluctuation. *J. Exp. Biol.* **200**, 9-18.
Wallingford, J. B. (2010). Planar cell polarity signaling, cilia and polarized ciliary beating. *Curr. Opin. Cell Biol.* **22**, 597-604.
Werner, M. E. and Mitchell, B. J. (2012). Understanding ciliated epithelia: the power of Xenopus. *Genesis* **50**, 176-185.
Whitfield, J. F. (2004). The neuronal primary cilium – an extrasynaptic signaling device. *Cell. Signal.* **16**, 763-767.
Yoshihiro, M., Keiko, W., Chieko, O., Akemi, K. and Baba, S. A. (1992). Regulation of ciliary movement in sea urchin embryos: Dopamine and 5-HT change the swimming behaviour. *Comp. Biochem. Physiol.* **101C**, 251-254.
Yu, X., Ng, C. P., Habacher, H. and Roy, S. (2008). Foxj1 transcription factors are master regulators of the motile ciliogenic program. *Nat. Genet.* **40**, 1445-1453.

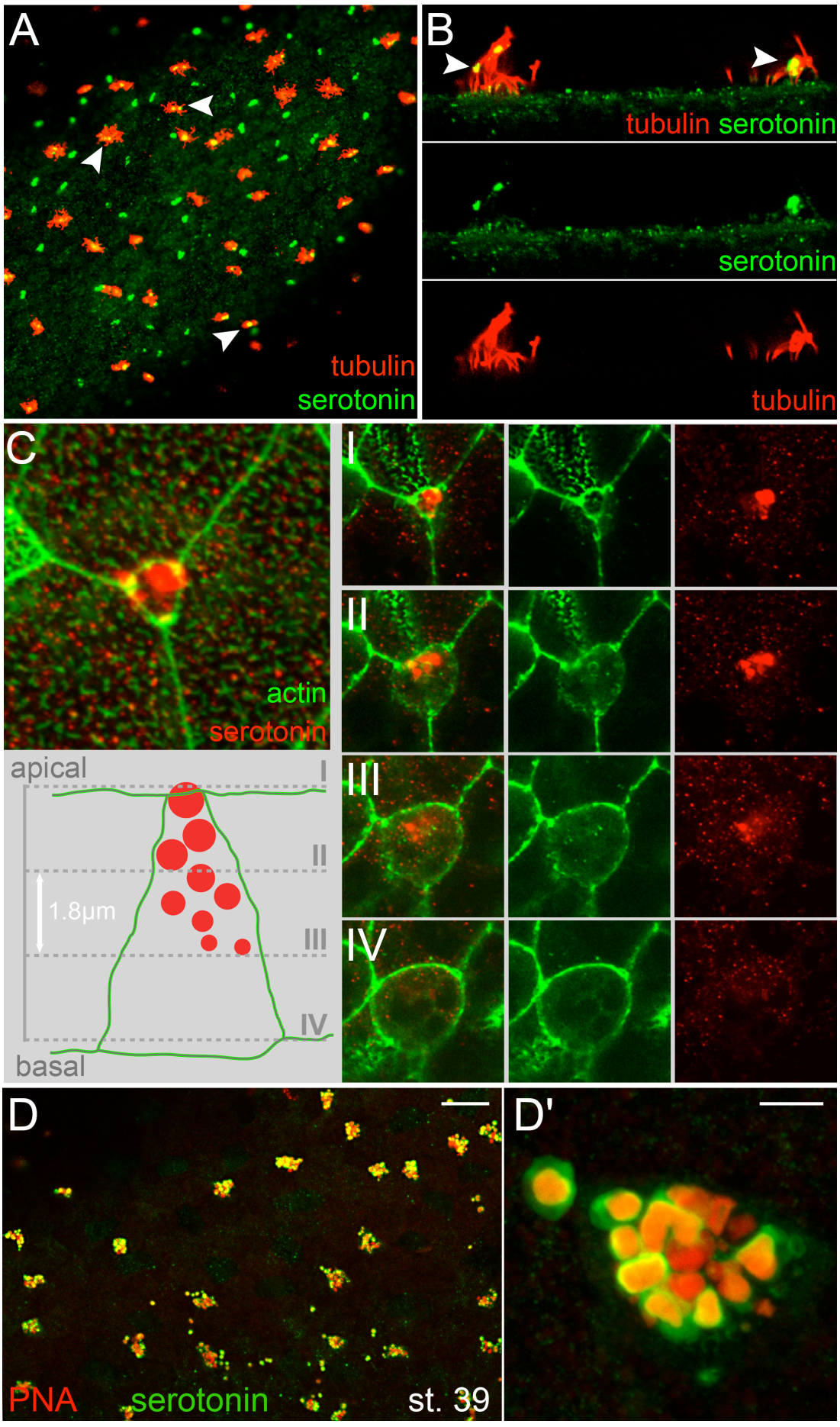
A
tubulin
serotonin
B
tubulin serotonin
serotonin
tubulin
C
actin
serotonin
apical
basal
1.8µm
I
II
III
IV
I
II
III
IV
D
PNA
serotonin
st. 39
D'

Fig. S1. Cilia association of serotonin-containing vesicles and vesicle maturation.

(A, B) Co-staining of serotonin (green) and cilia (red; anti acetylated- -tubulin) at stage 32 reveals occasional co-localization in the epidermis (white arrowheads). (**B**) Higher magnification of two MCCs in side view. Note the vesicular nature of serotonin staining in all cases. **(C)** Vesicle maturation in SSCs. Z-stack analysis of a single SSC stained for serotonin (red) and actin (phalloidin, green). Apical to basal horizontal optical sections (I-V) were used to reconstruct an orthogonal hypothetical model of vesicle maturation (lower panel in C). Vesicles localized basally were small (0.2 μm diameter), with a continuous increase in diameter to a maximum of 1 μm towards the apical pole of the cell. **(D, D')** Vesicular co-localization of serotonin (green) and peanut agglutinin (PNA; red) in the epidermis of *Xenopus laevis* tadpoles at stage 39. Scale bars in (D) and (D') represent 50 and 5μm, respectively.

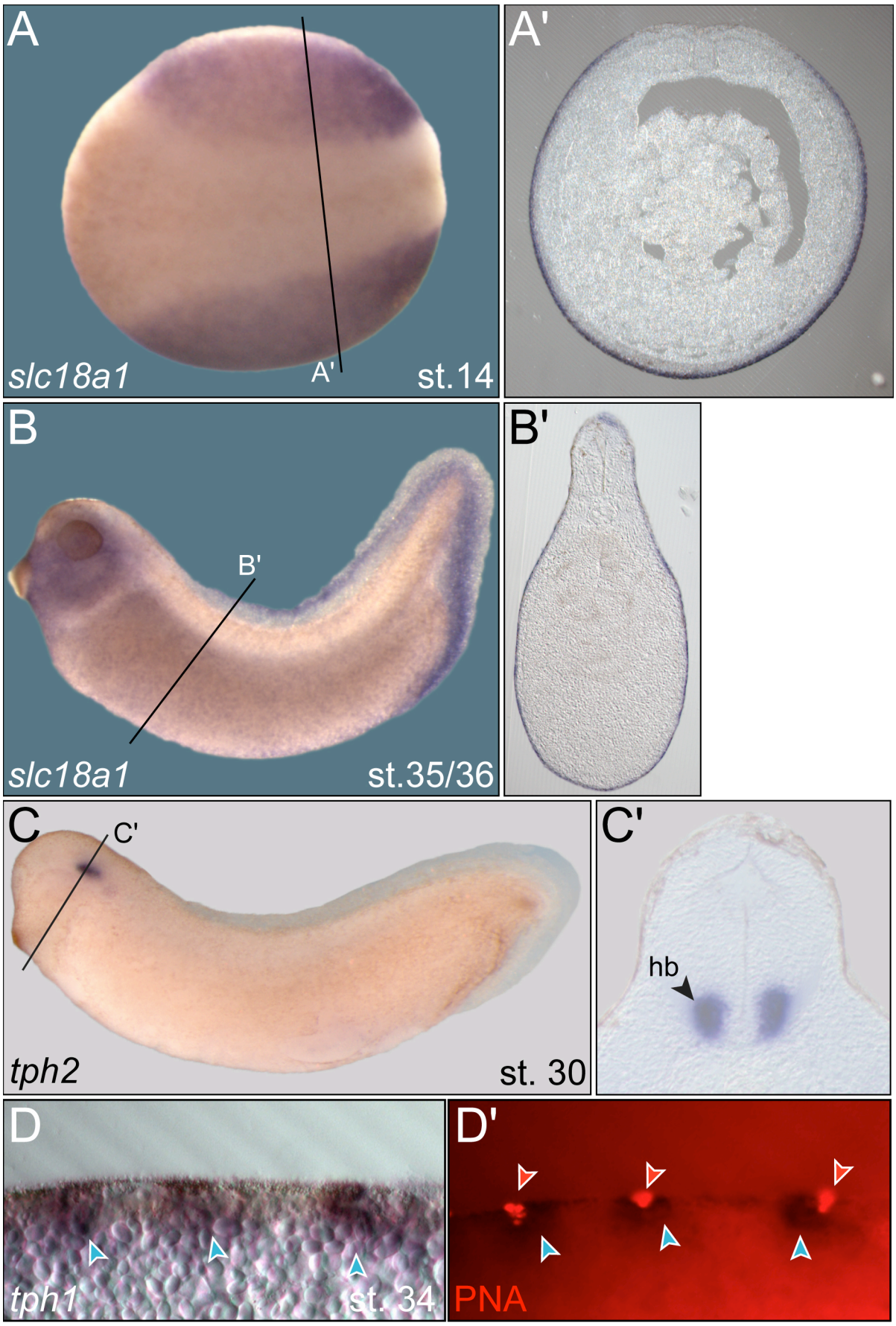

Fig. S2. Embryonic expression of serotonin pathway components.

(A, B) Epidermal expression of monoamine transporter *slc18a1* mRNA in stage 14 neurula (A) and stage 35/36 tadpole (B) embryos. Transverse sections (A', B') reveal uniform superficial staining in the epidermis. Note lack of expression in the neural plate at stage 14. **(C)** *tph2* expression was restricted to the hindbrain at stage 30. (C') Transverse histological section. Embryos are shown in lateral views except for panel (A), which shows a dorsal perspective. **(D, D')** *tph1* mRNA expressing SCCs (blue arrowheads) secrete PNA positive vesicles (red arrowheads). (D) Close-up bright field image of a transverse section of a *tph1* stained tadpole at stage 36 displaying three SSCs. (D') Fluorescent PNA signals (red) co-localize with *tph1* mRNA.

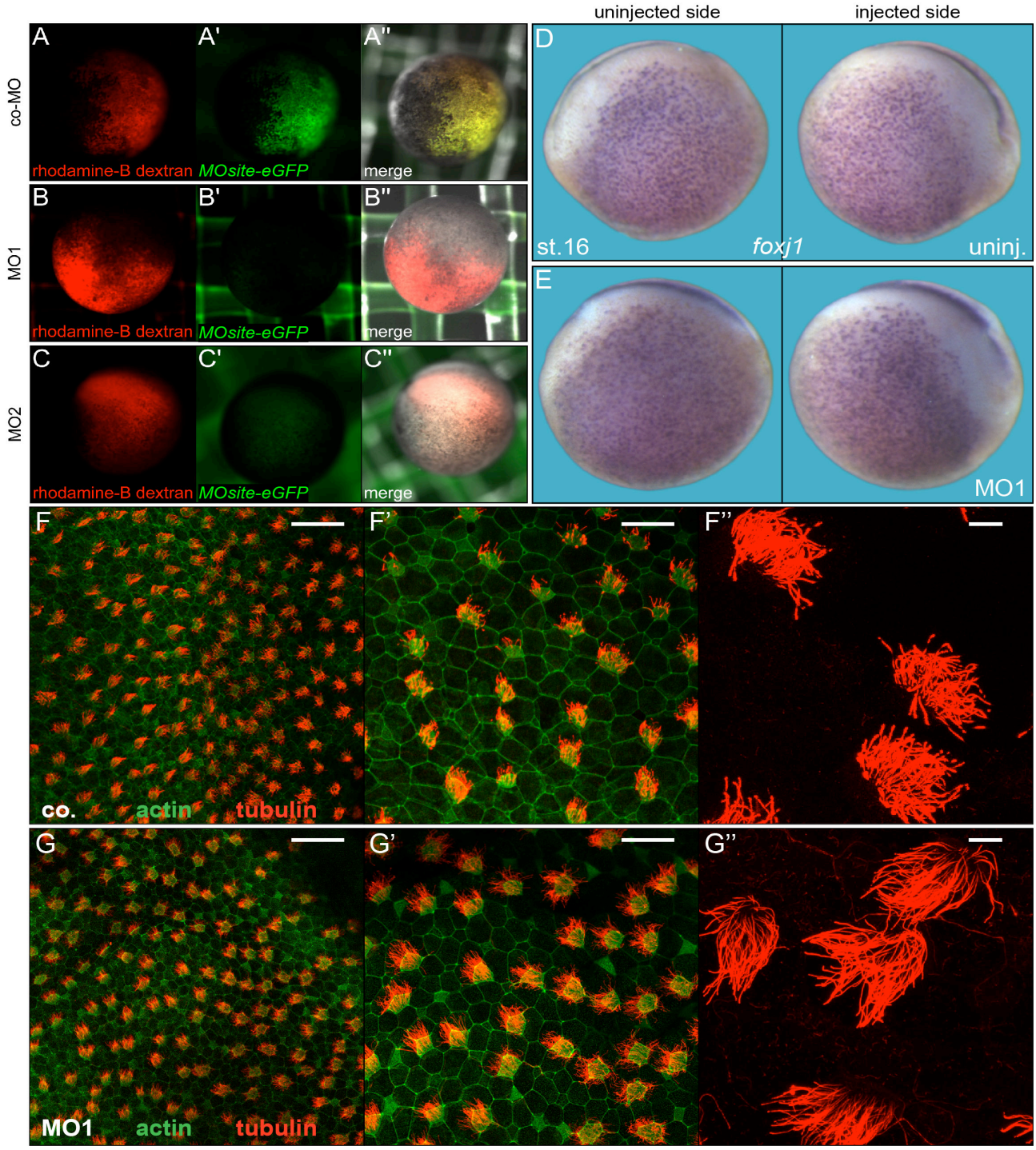

Fig. S3. MO-specificity, *foxj1* expression and ciliogenesis in *Htr3* morphants.

(A-C) MO specificity. MO1 and MO2 specificity was tested using an eGFP-reporter construct. A 60 bp fragment of *Htr3* including the translational start site as well as bindings sites for both MO1 and MO2 (cf. Fig. 1C) was cloned in frame with eGFP (cf. Gessert et al., 2010). Injection into animal blastomeres of 4-cell embryos were performed using rhodamine-B dextran as lineage tracer. (**A**) Co-injection of co-MO did not affect green fluorescence of reporter construct in targeted

regions at stage 9. (**B**, **C**) Absence of green fluorescence upon co-injection of MO1 (B) or MO2 (C) demonstrated MO-specificity.

(D, E) Unaltered *foxj1* mRNA expression in the frog epidermis of *Htr3* morphant. Embryos shown in lateral view, anterior to the left. **(F, G)** Wildtype and morphant epidermis at stage 34 stained for cilia (red) and actin (green) using anti-acetylated-α-tubulin antibodies and phalloidin. MCC number and ciliation were unaffected in morphants (F', G', F'', G''). Increasing magnifications. Scale bars represent 100µm (F, G), 50µm (F', G') and 10µm (F'', G'').

Movie S1. Inhibition of serotonin synthesis reduces velocity of cilia driven mucus flow.

Time-lapse movies (10 seconds at 28.5 fps), showing transport of fluorescent beads at the epidermis of stage 32 tadpole embryos, which were either untreated (control) or incubated with 100µM TPH inhibitor PCPA alone or in combination with 1mM serotonin. Mean and relative (in % of control) velocity of bead movements are indicated.

Movie S2. Low mucus flow velocity in *Htr3* morphant embryos.

Time-lapse movies (10 seconds at 28.5 fps) show transport of fluorescent beads at the epidermis of stage 32 tadpoles. Specimens were untreated (control), injected with MO1 alone, with MO1 and a mutated *Htr3* mRNA (rescue), or with MO2 alone. Mean and relative (% of control) velocity of bead movements are indicated.

Movie S3. Serotonin signaling controls ciliary motility in the tadpole epidermis.

Time-lapse movies (1.7 sec; 0.22 x real time), displaying ciliary motility on wildtype MCCs (left; control), and reduced motility (middle) or virtually immotile cilia (right) in *Htr3* morphants (cf. Fig. 4D). Cilia were visualized by co-injection of 800 pg mRFP mRNA.

Supplemental reference:

Gessert, S., Bugner, V., Tecza, A., Pinker, M. and Kühl, M. (2010). FMR1/FXR1 and the miRNA pathway are required for eye and neural crest development. *Dev Biol* **341**, 222–235.

Movie 1.

Movie 2.

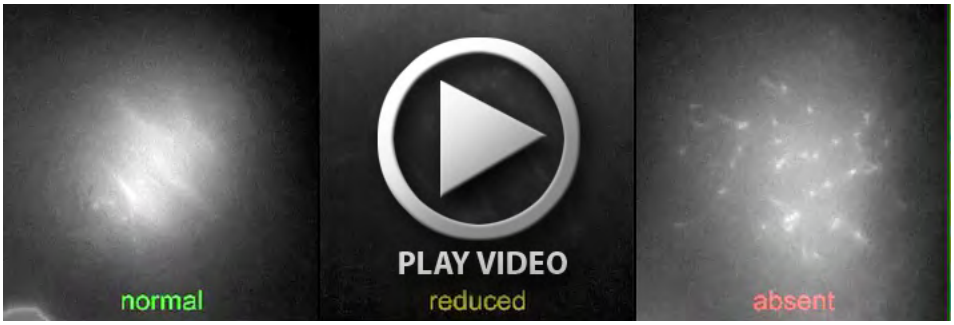

Movie 3.